Supporting Information

Electronic Conductance and Thermopower of Single-molecule Junctions of Oligo(phenyleneethynylene) Derivatives

Hervé Dekkiche, Andrea Gemma, Fatemeh Tabatabaei, Andrei S. Batsanov, Thomas Niehaus, Bernd Gotsmann and Martin R. Bryce

Table of contents

I) Experimental details for the synthesis of the OPE3 molecules

General procedure for the Sonogashira coupling reactions

A solution containing the diiodide (1 eq.) in a THF/iPr$_2$NH mixture (5/1 v/v, 4 mL per 0.1 mmol eq.) was degased by bubbling argon for 20-30 min. Catalytic amounts of Pd(PPh$_3$)$_2$Cl$_2$ (0.05 eq.) and CuI (0.05 eq.) were added, followed by 4-acetynyl-dihydrobenzo[b]thiophene (2.2 eq.). The mixture was then stirred at room temperature for 2 h and the solvents were evaporated under reduced pressure in the presence of a few spatulas of silica. The resulting residue was then chromatographed using CH$_2$Cl$_2$/n-hexane on silica to extract the desired products. After removal of the solvents, the compounds were precipitated from a CH$_2$Cl$_2$ solution and dried under vaccum after filtration and washing with n-hexane.

Synthesis of OPE3-Ph
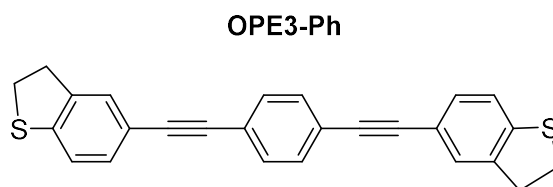
OPE3-Ph

Starting from 1,4-diiodobenzene **I$_2$-Ph** (51 mg, 154 μmol), **OPE3-Ph** was obtained (28 mg, 71 mmol, 46 %) following the general procedure. Eluent for column chromatography: n-hexane /CH$_2$Cl$_2$ (1.5:1 v/v).

^{1}HNMR (400 MHz, CDCl$_3$), δ (ppm) 7.46 (s, 4H, H$_{Ar-Ph}$), 7.34 (d, 1.7 Hz, 2H, H$_{Ar-DHBT}$), 7.29 (dd, J = 8.0, 1.7 Hz, 2H, H$_{Ar-DHBT}$), 7.19 (d, J = 8.0 Hz, 2H, H$_{Ar-DHBT}$), 3.42 – 3.87 (m, 4H, CH$_{2-DHBT}$), 3.31 – 3.28 (m, 4H, CH$_{2-DHBT}$).

^{13}CNMR (100 MHz, CDCl$_3$), δ (ppm) 143.04, 140.55, 131.53 (CH$_{Ph}$), 130.98 (CH$_{DHBT}$), 127.38 (CH$_{DHBT}$), 123.19, 122.13 (CH$_{DHBT}$), 118.74, 91.60, 88.81, 36.00 (CH$_2$), 33.61 (CH$_2$).

HR-MS (ASAP), m/z calcd for C$_{28}$H$_{18}$S$_2$: 395.0928. Found for [M+H]$^+$: 395.0925.

UV-Vis (dichloromethane), λ$_{max}$ (nm): 351 and 371.

X-Ray: Crystals grown from dichloromethane/MeOH, size: 0.49 × 0.22 × 0.09 mm, T=120 K, monoclinic, space group P2$_1$/c, a = 12.3046(10) Å, b = 8.9443(8) Å, c = 9.1320(7) Å, β = 98.241(7)°, V = 994.65(14) Å^3, Z = 2, 2θ ≤ 55°, 9448 reflections collected (2287 independent), R$_1$ = 0.048 on 1848 reflections with I≥2σ(I), wR$_2$ = 0.138 on all data. CCDC-1996615.

Synthesis of OPE3-Ph(OMe)₂
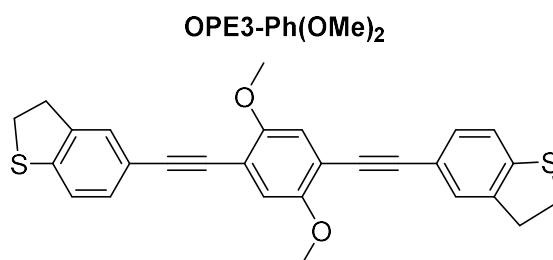
OPE3-Ph(OMe)$_2$

Starting from 1,4-diiodo-2,5-dimethoxybenzene **I₂-Ph(OMe)₂** (91 mg, 234 μmol), **OPE3-Ph(OMe)₂** was obtained (55 mg, 121 μmol, 52%) following the general procedure. Eluent for column chromatography: *n*-hexane /CH$_2$Cl$_2$ (1.5:1 v/v) gradient to *n*-hexane /CH$_2$Cl$_2$ (1:2 v/v).

^{1}HNMR (400 MHz, CDCl$_3$), δ (ppm) 7.38 (d, J = 1.7 Hz, 2H, H$_{Ar-DHBT}$), 7.32 (dd, J = 8.0 Hz, 1.7 Hz, 2H, H$_{Ar-DHBT}$), 7.18 (d, J = 8.0 Hz, 2H, H$_{Ar-DHBT}$), 7.00 (s, 2H, H$_{Ph}$), 3.89 (s, 6H, O-CH$_3$), 3.41 – 3.37 (m, 4H, CH$_{2-DHBT}$), 3.31 – 3.27 (m, 4H, CH$_{2-DHBT}$).

^{13}CNMR (100 MHz, CDCl$_3$), δ (ppm) 153.92, 142.91, 140.45, 131.04 (CH$_{DHBT}$), 127.46 (CH$_{DHBT}$), 122.06 (CH$_{DHBT}$), 118.91, 115.62 (CH$_{Ph}$), 113.45, 95.44, 85.33, 56.60 (CH$_3$), 35.98 (CH$_2$), 33.60 (CH$_2$).

HR-MS (ASAP), *m/z* calcd for C$_{28}$H$_{22}$O$_2$S$_2$:454.1061. Found for [M]$^+$: 454.1065.

UV-Vis (dichloromethane), λ$_{max}$ (nm): 330, 380 and 395.

Synthesis of OPE3-An
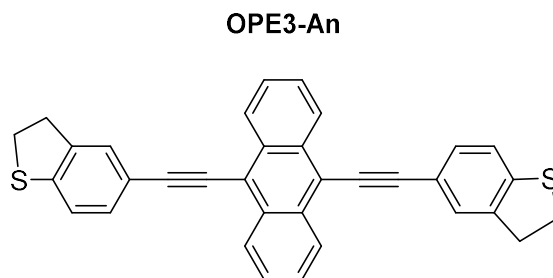
OPE3-An

Starting from 9,10-diiodoanthracene **I₂-An** (67 mg, 156 μmol), **OPE3-An** was obtained (37 mg, 75 μmol, 48 %) following the general procedure. Eluent for column chromatography: *n*-hexane /CH$_2$Cl$_2$ (1.5: 1 v/v). Special care was taken to perform all the reaction and purification steps in the absence of day- and UV-light.

^{1}HNMR (400 MHz, CDCl$_3$), δ (ppm) 8.69 – 8.61 (m, 4H, H$_{An}$), 7.65 – 7.61 (m, 4H, H$_{An}$), 7.59 (d, J = 1.7 Hz, 2H, H$_{Ar-DHBT}$), 7.54 (dd, J = 8.0, 1.7 Hz, 2H, H$_{Ar-DHBT}$), 7.29 (d, J= 1.7 Hz, 2H, H$_{Ar-DHBT}$), 3.44 – 3.34 (m, 8H, CH$_{2-DHBT}$).

^{13}CNMR (100 MHz, CDCl$_3$), δ (ppm) 143.40, 140.76, 132.14, 131.04 (CH$_{DHBT}$), 127.41 (CH$_{An}$ + CH$_{DHBT}$), 126.84 (CH$_{An}$), 122.30 (CH$_{DHBT}$), 119.13, 118.56, 102.90, 86.30, 36.06 (CH$_2$), 33.69 (CH$_2$).

HR-MS (ASAP), *m/z* calcd for C$_{34}$H$_{22}$S$_2$: 495.1241. Found for [M+H]$^+$: 495.1220.

UV-Vis (dichloromethane), λ_{max} (nm): 277, 321, 334, 460 and 489.

X-Ray: Crystals grown from dichloromethane/*n*-hexane, size : 0.57 × 0.45 × 0.17 mm, T=120 K, monoclinic, space group P2$_1$/c, a = 9.7811(4) Å, b = 23.2361(11) Å, c = 11.2452(5) Å, β = 108.171(2)°, V = 2428.29 (19) Å^3, Z = 4, 2θ ≤ 60°, 57742 reflections collected (7116 independent), R$_1$ = 0.0465 on 5256 reflections with I≥2σ(I), wR$_2$ = 0.125 on all data. CCDC-1996616.
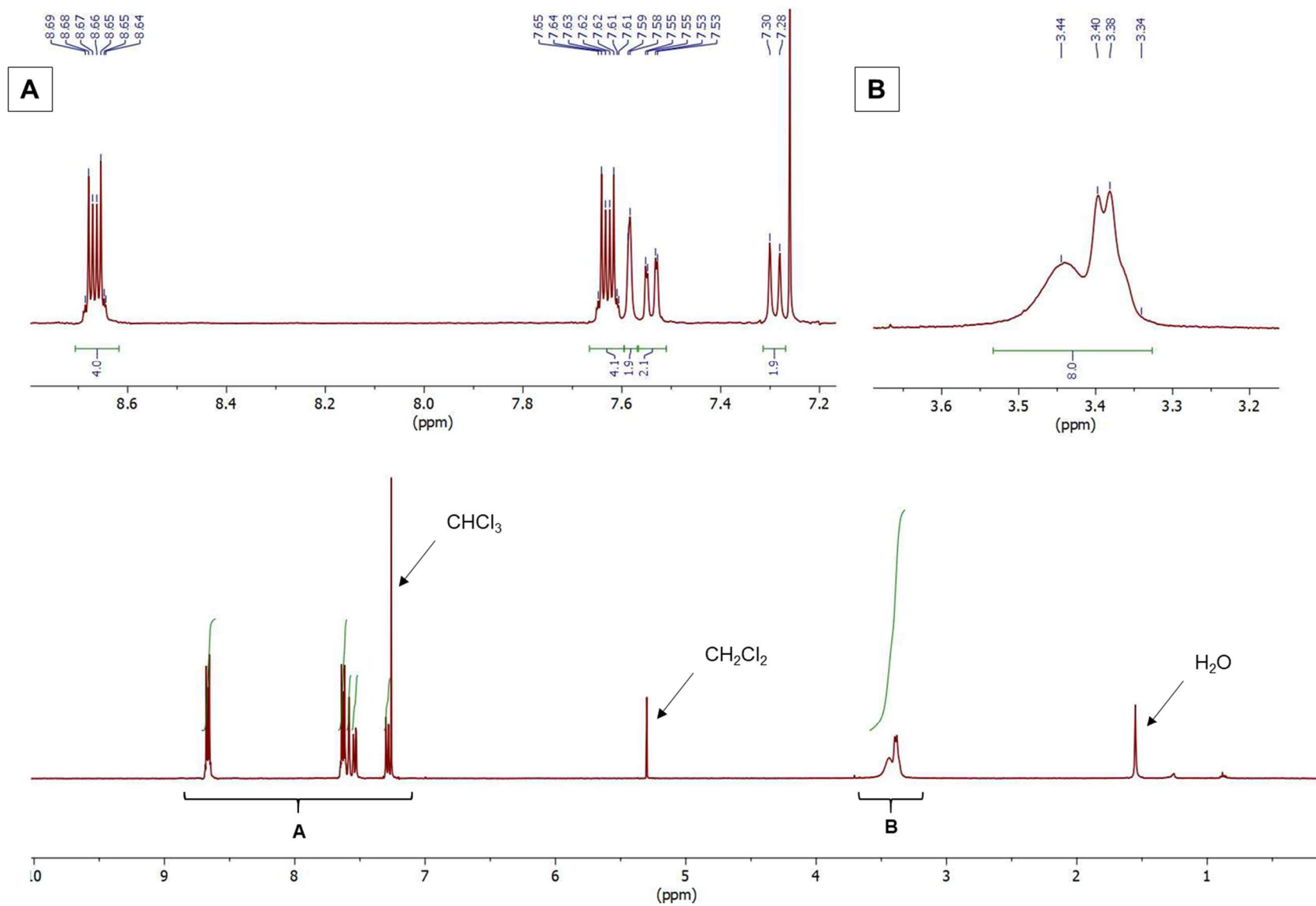
II) Characterisation data

^{1}H NMR
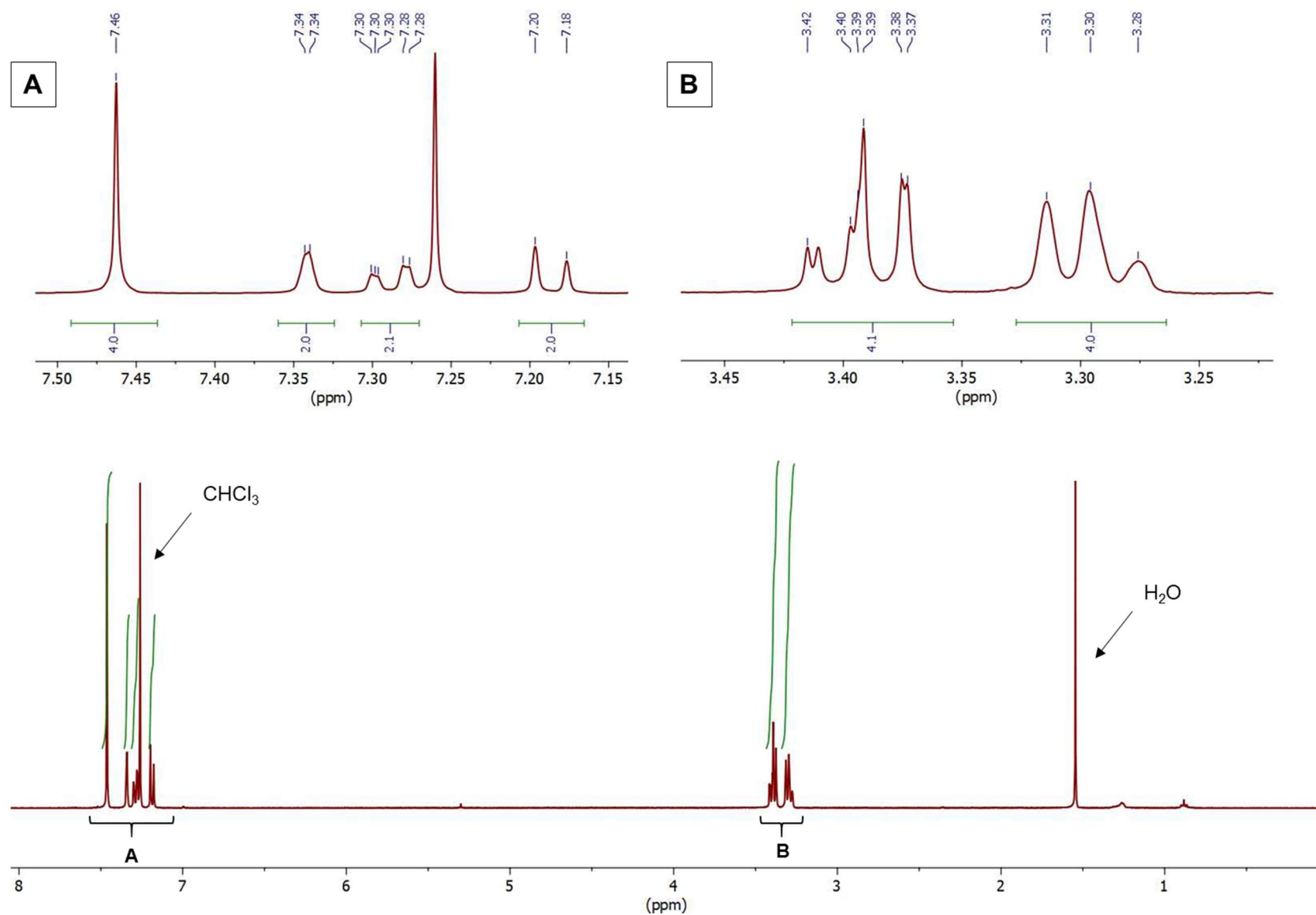
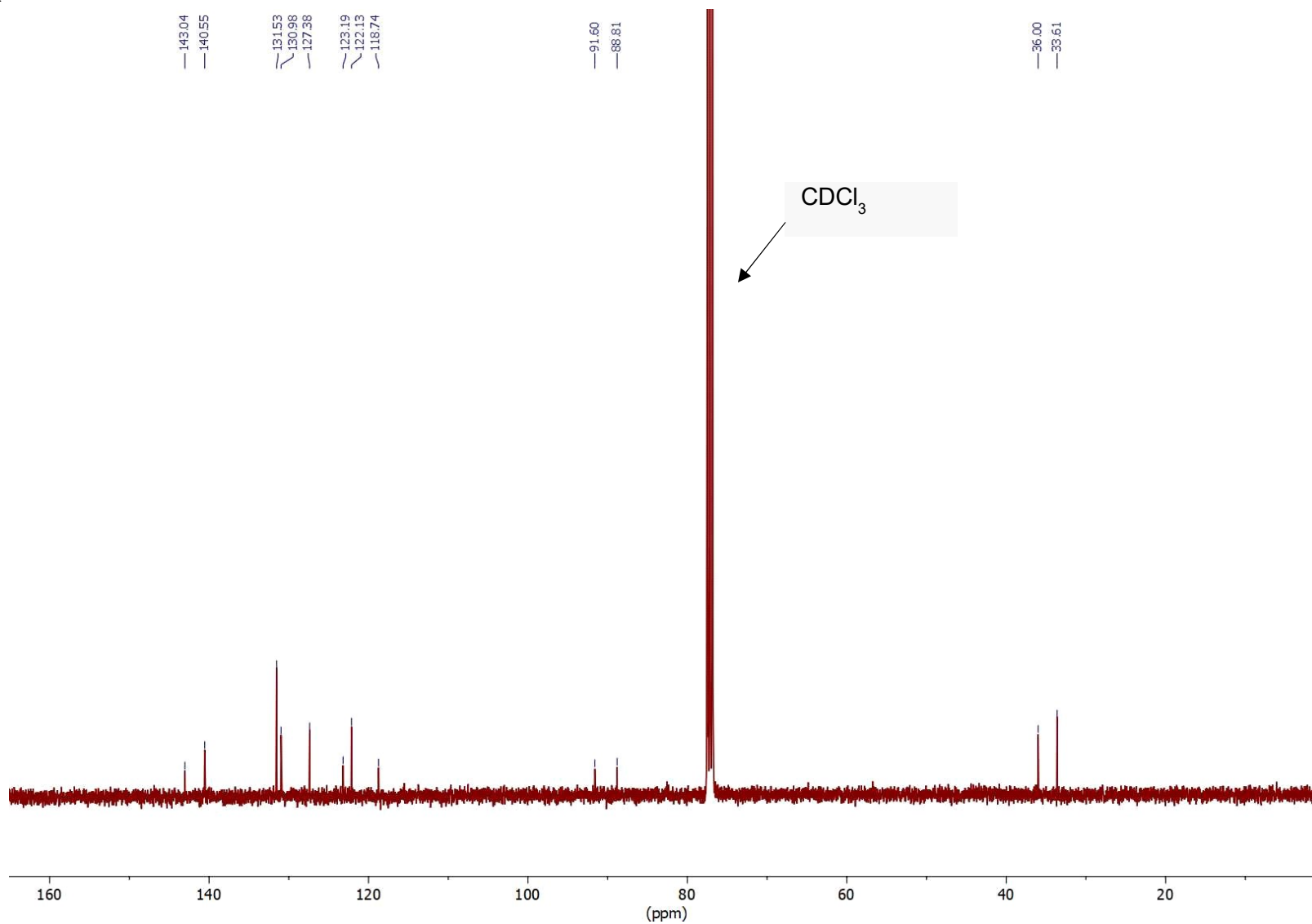**Figure 1.** ^{1}H NMR spectrum of **OPE3-Ph** (400 MHz, CDCl$_3$ at 25 °C).
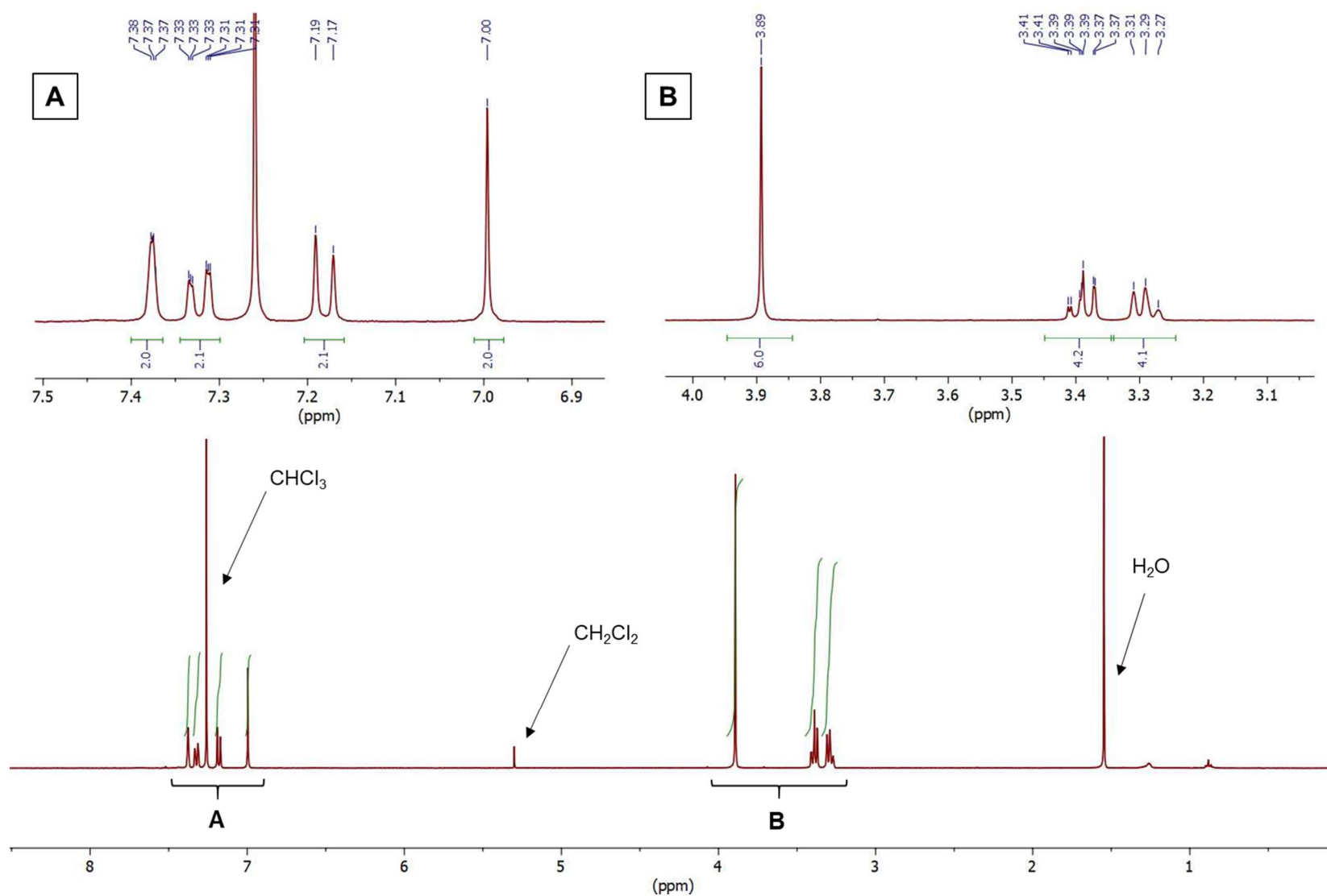
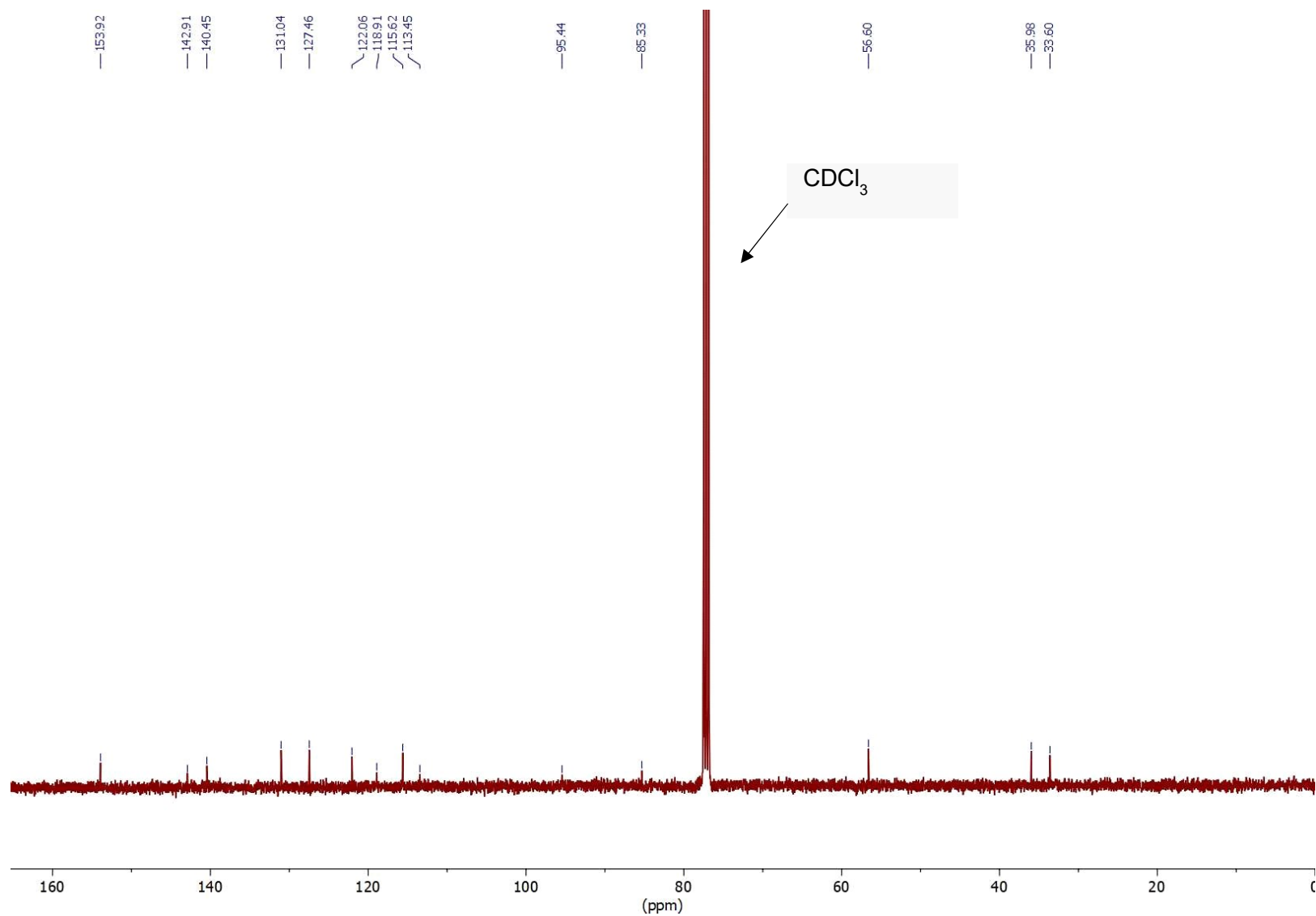**Figure 2.** ^{1}H NMR spectrum of **OPE3-Ph(OMe)$_2$** (400 MHz, CDCl$_3$ at 25 °C).

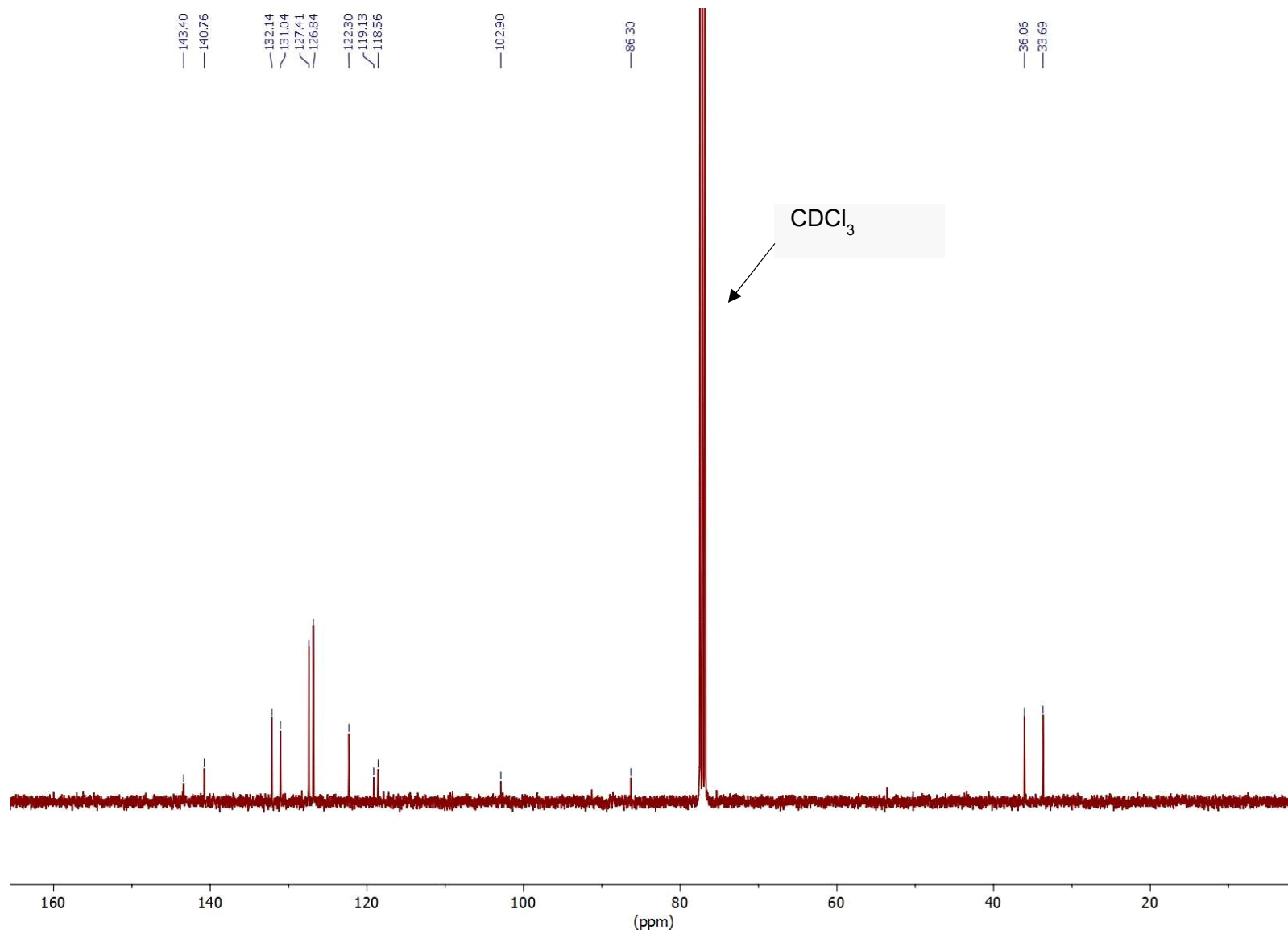**Figure 3.** ^{1}H NMR spectrum of **OPE3-An** (400 MHz, CDCl$_3$ at 25 °C).

¹³C NMR

Figure 4. ¹³C NMR spectrum of **OPE3-Ph** (100 MHz, CDCl₃ at 25 °C).

Figure 5. ^{13}C NMR spectrum of **OPE3-Ph(OMe)₂** (125 MHz, CDCl₃ at 25 °C).

Figure 6. ¹³C NMR spectrum of **OPE3-An** (125 MHz, CDCl₃ at 25 °C).

Mass spectrometry
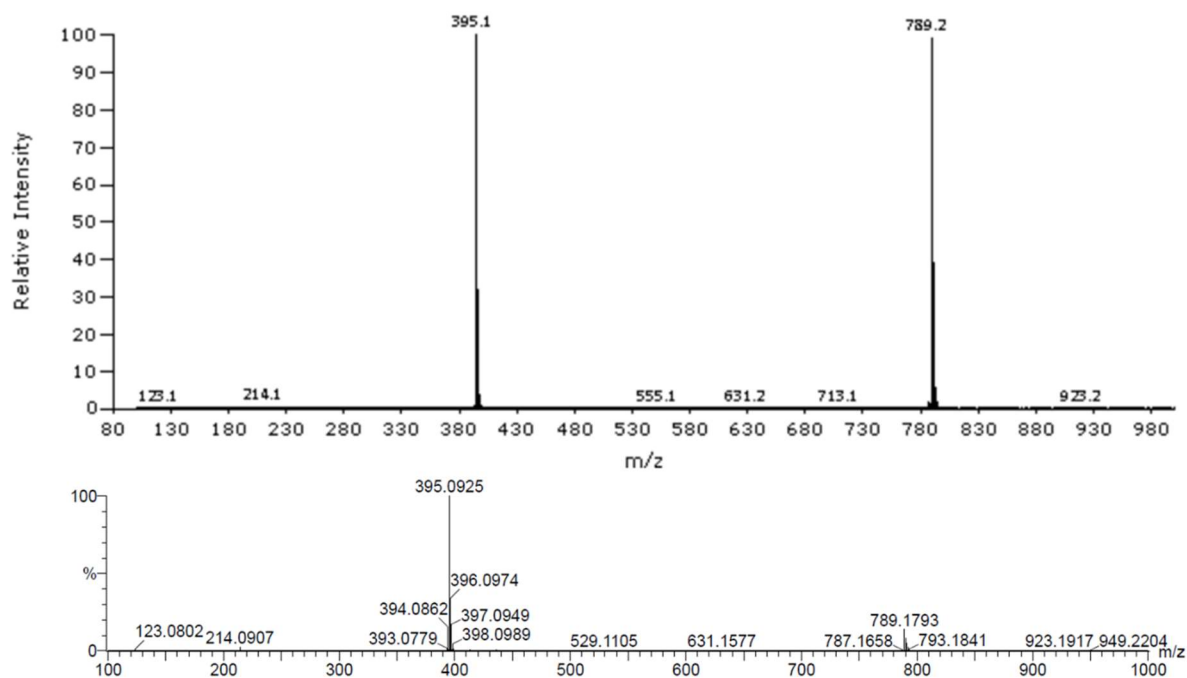
Figure 7. Mass spectrum and high-resolution profile obtained for **OPE3-Ph** (ASAP).
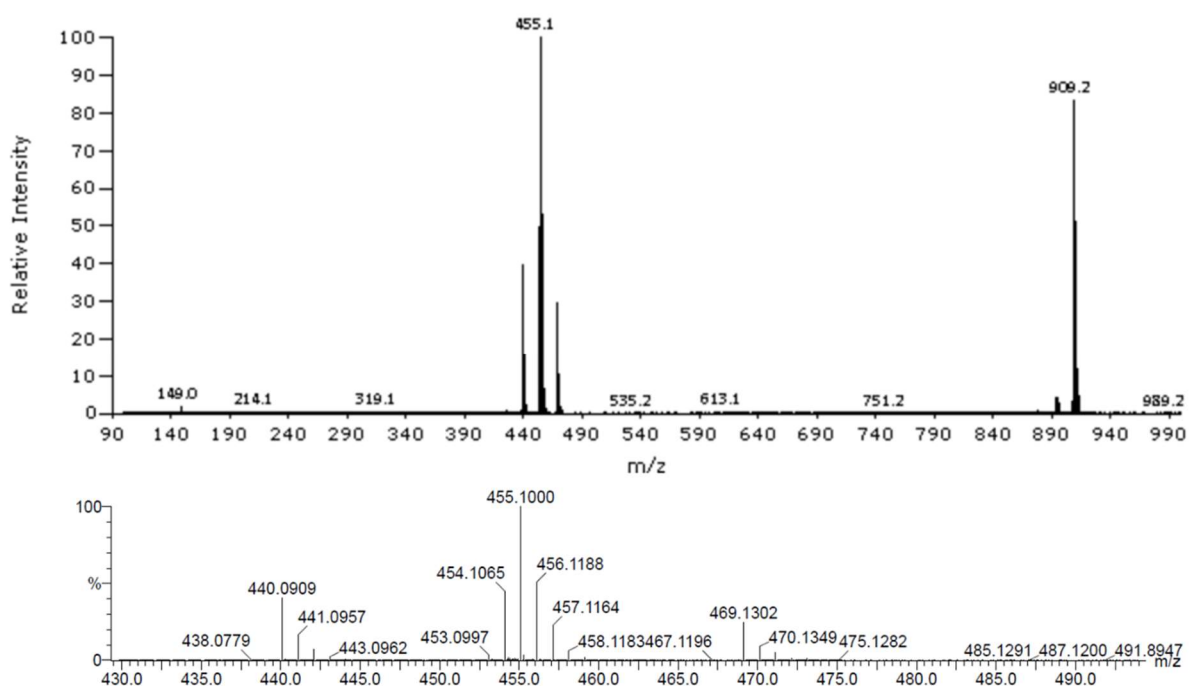
Figure 8. Mass spectrum and high-resolution profile obtained for **OPE3-Ph(OMe)$_2$** (ASAP) ; Signals above and below the compound peaks are attributed to degradation products (reaction with ambient air and O-demethylation, respectively).
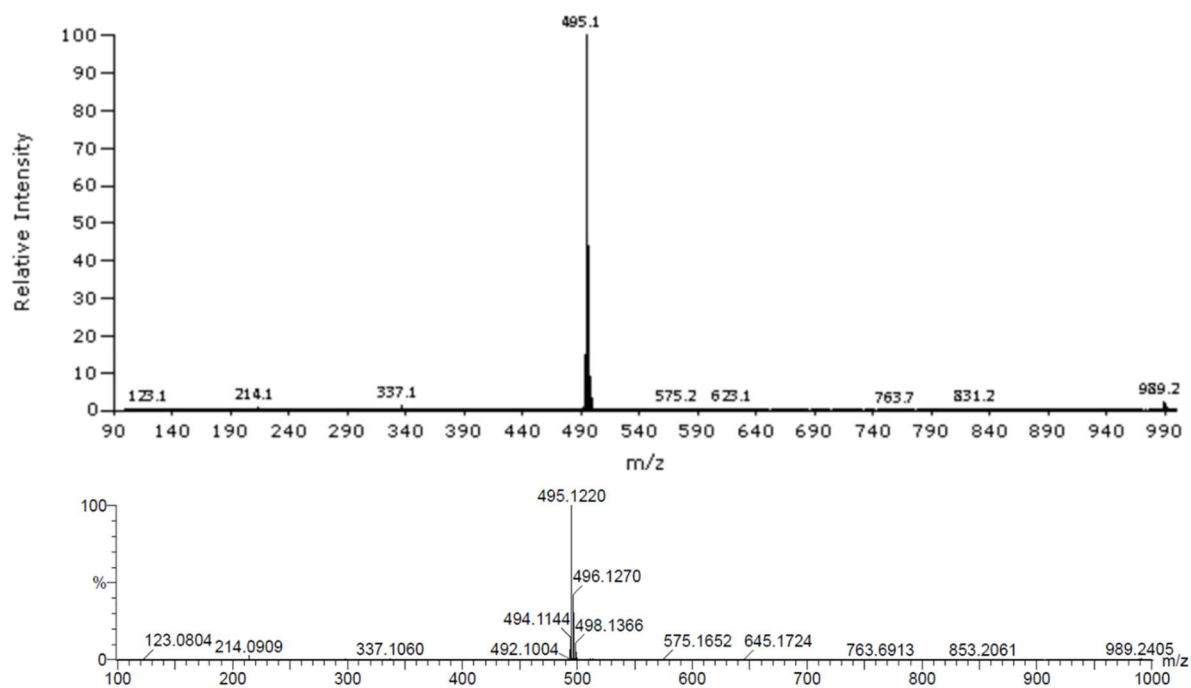
Figure 9. Mass spectrum and high-resolution profile obtained for **OPE3-An** (ASAP).

Optical spectroscopy

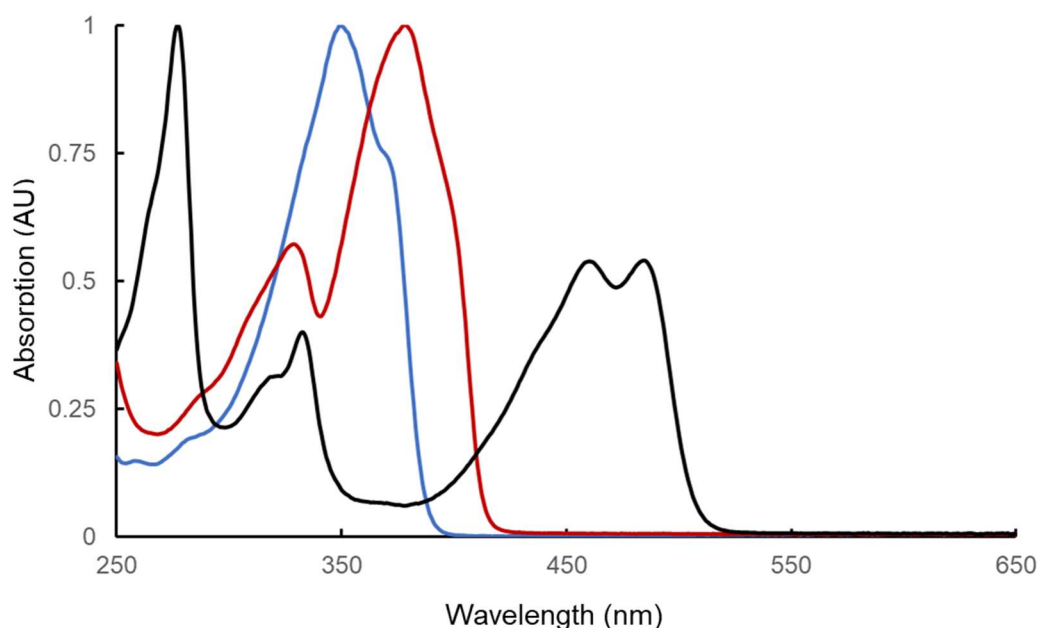**Figure 10.** Normalised UV-vis absorption spectra of **OPE3-Ph** (blue), **OPE3-Ph(OMe)₂** (red) and **OPE-An** (black) recorded in dichloromethane at 298 K. The concentration of the samples was in the range of 0.01-0.0025 mg/mL. The absorption onsets are at 371, 395 and 489 nm for **OPE3-Ph**, **OPE3-Ph(OMe)₂** and **OPE-An**, which correspond to energies of 3.342, 3.038 and 2.454 eV respectively according to the formula E = 1240/λ(nm).
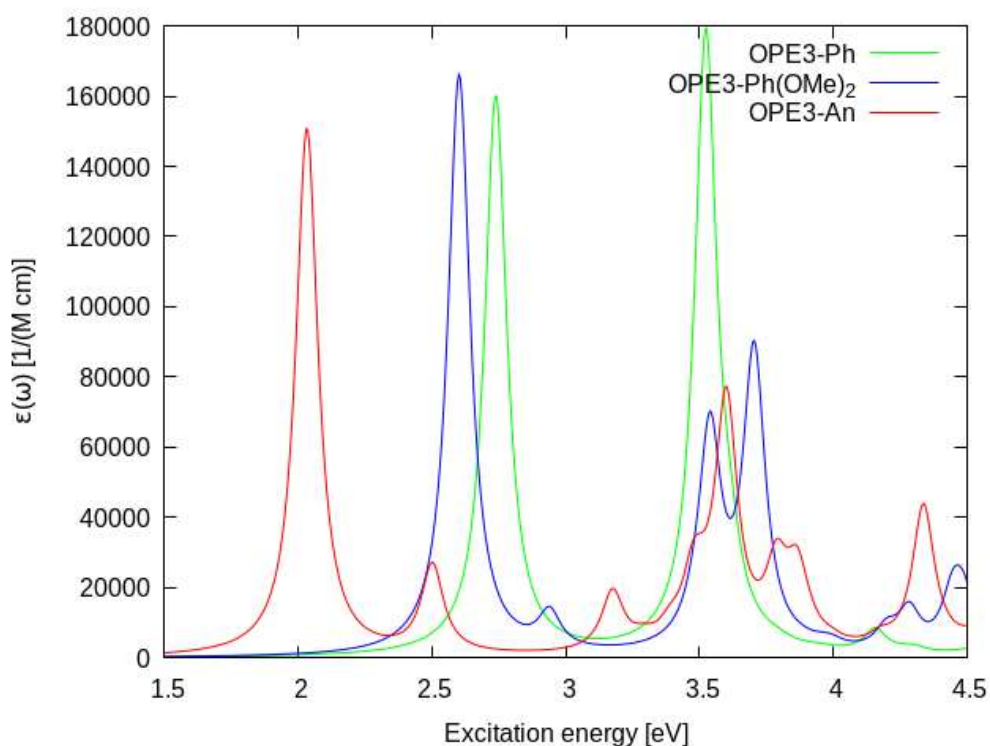
Figure 11. TD-DFTB absorption spectra of OPE3 derivatives in the gas phase. Absorption peaks have been Lorentzian broadened by 0.1 eV. Structures are optimized at the DFTB level.

As a further characterisation we recorded the UV-Vis absorption spectra of **OPE3-Ph**, **OPE3-Ph(OMe)₂** and **OPE3-An** in dichloromethane solution (Fig. 10) and compared them to simulated spectra (Fig. 11). The position of the absorption maxima are following a similar trend in both cases. Better agreement over the full wavelength range can be obtained, but requires more sophisticated exchange-correlation functionals in the DFTB treatment. Please note that due to electron-hole interactions, the optical gap generally differs strongly from the frontier orbital (HOMO-LUMO) gap that is relevant for transport.

III) Crystal structures: packing diagrams

OPE3-Ph
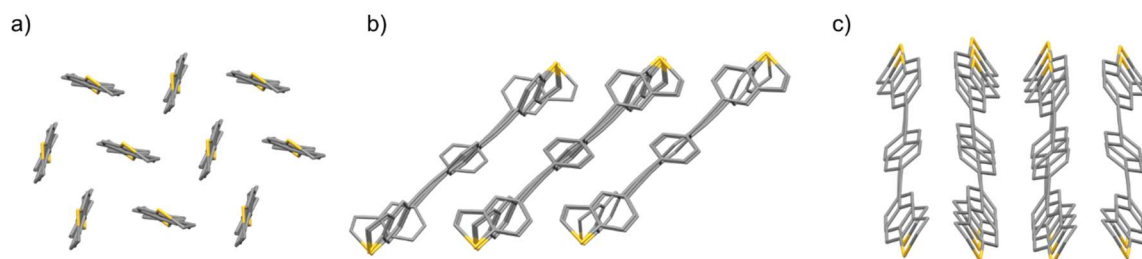
Figure 12. a) top, and b) and c) side views of **OPE3-Ph** packing in its crystal structure.
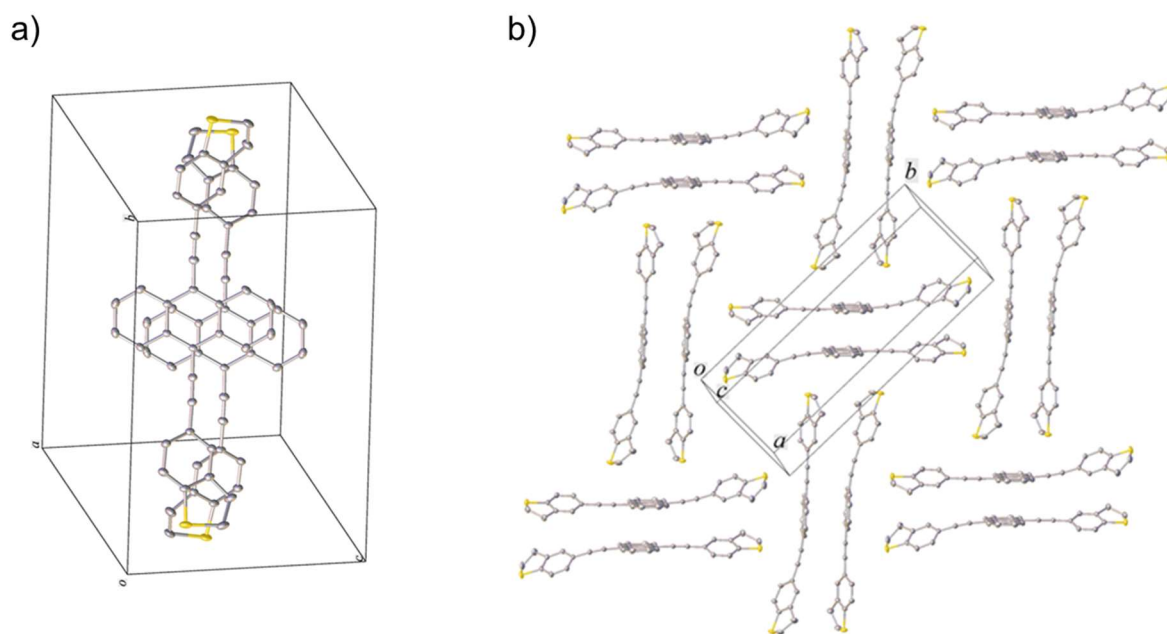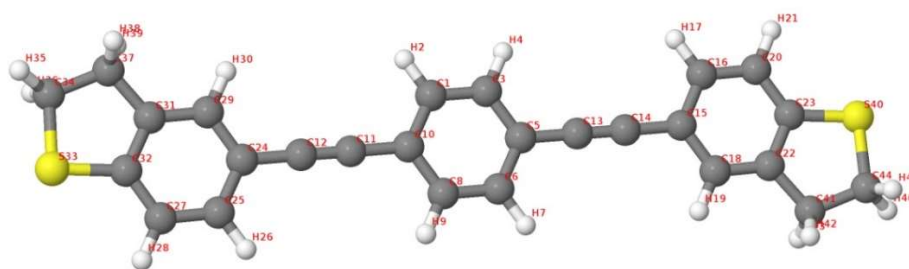
OPE3-An

Figure 13. a) dimeric structure adopted by **OPE3-An** in its crystal unit cell and b) packing view

IV) Structural investigations by DFT

Figure 14. Structure of **OPE3-Ph** with atom labels.

| Geometrical parameter	Exp. crystal structure	Isolated gas phase[A]	Au$_{20}$ –**OPE3-Ph** complex[B]	**OPE3-Ph-**surface (tilted)[C]	**OPE3-Ph-**surface (straight)[D]
S40-C23 [Å]	1.75	1.77	1.79	1.77	1.77
C13 – C14 [Å]	1.22	1.23	1.23	1.22	1.22
Au – S40 [Å]	-	-	2.56	2.55	2.77
C13 – C14 – C15 [deg]	178.9	179.9	176.6	179.2	171.9
C44 – S40 – C23 [deg]	92.9	90.7	90.7	91.0	91.0
C44 – S40 – Au [deg]	-	-	103.3	108.7	107.3
S40 – C23 – C20 – C16 [deg]	179.6	179.7	172.4	178.5	172.1
Surface - **OPE3-Ph** plane [deg]	-	-	53.9	33.2	83.4

Table 1: Representative geometrical parameters for **OPE3-Ph** including distances, angles and dihedral angles. **A: OPE3-Ph** in the gas phase, PBE/6-31G*, NWChem, **B:** Au$_{20}$-**OPE3-Ph**-Au$_{20}$ complex in the gas phase, PBE/6-31G*/lanl2dz_ecp, NWChem, **C: OPE3-Ph**-Au(111) (flat surface), lowest energy conformer at top position, PBE/PW, Quantum ESPRESSO, **D: OPE3-Ph**-Au(111) (flat surface), higher energy conformer at top position, PBE/PW, Quantum ESPRESSO.

The experimental crystal structure, results of the planar surface DFT relaxations and all junction models for which transport calculations have been performed are freely available under the DOI: 10.5281/zenodo.3975842 at zenodo.org.

V) Additional transport simulations
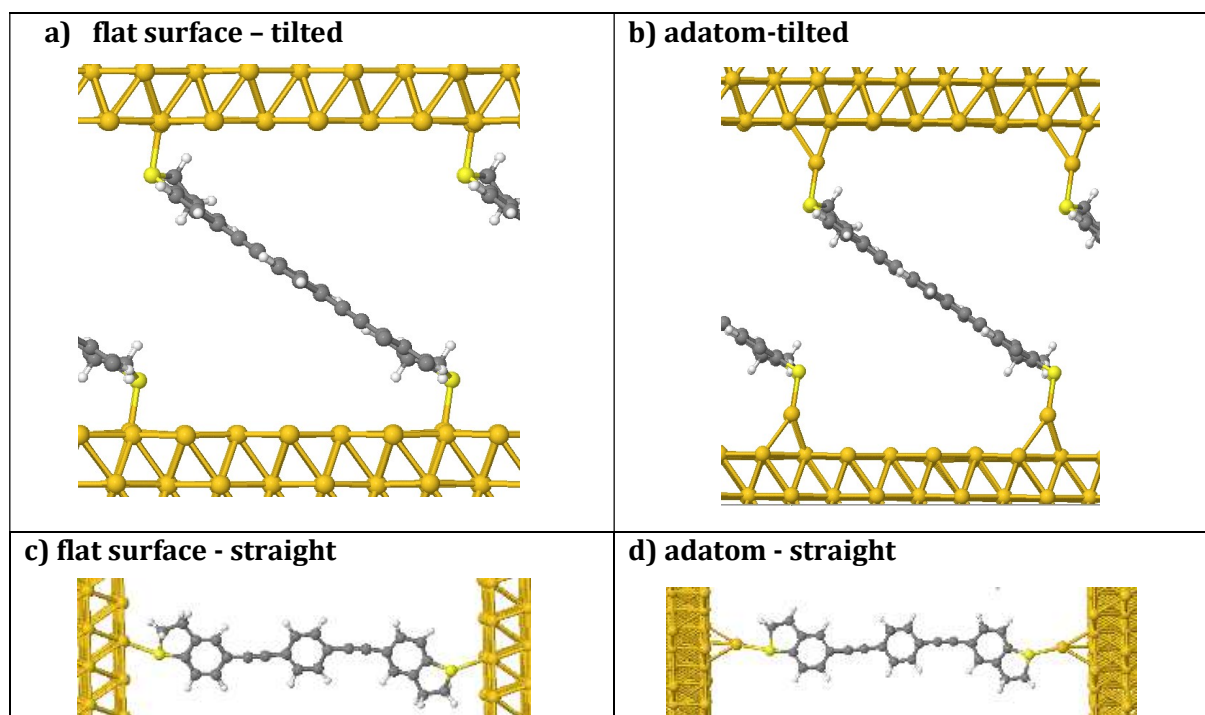
Figure 15.   Possible **OPE3-Ph** junction configurations.

We performed additional transport simulations for **OPE3-Ph** to investigate the influence of the metal-molecule binding. The computational parameters are the same as detailed in the main article. There, the junction was constructed by first optimizing a Au_{20}-molecule-Au_{20} complex in the gas phase which was then embedded in the junction. We refer to this conformer as **Au20-tilted** (main article Fig. 6). Four additional structures are considered here: the first one is based on the top conformer obtained in the periodic DFT calculations (see main article Fig 5a)), where **OPE3-Ph** binds directly to a flat gold surface. Due to limited computational resources, the second electrode is manually placed in a symmetrical fashion with respect to the first electrode without additional geometry relaxations (**flat surface – tilted,** Fig. 15a)). The periodic DFT calculations also predict another stable conformer in a top position which is higher in energy, where the molecule is oriented perpendicular to the surface. The corresponding junction model is named (**flat surface – straight**, Fig. 15c)). We also consider binding through adatoms. Both hcp and fcc positioning of the adatom were considered, but since the resulting transmission differs only very slightly, only fcc results are shown. Calculations for straight (**adatom – straight**, Fig. 15d)) and tilted orientations of **OPE3-Ph** with respect to the adatom have been performed (**adatom – tilted**, Fig. 15b)).

The resulting transmission (Fig. 16) is found to be rather noisy around the Fermi energy, which is related to manual construction of the junctions without proper geometry relaxation. Some general trends can nevertheless be found. The straight conformers feature HOMO/LUMO resonances that are considerably shifted to higher energies with respect to **Au20-tilted** and therefore lead to positive Seebeck coefficients. The adatoms have an opposite effect, such that the **adatom – tilted** conformer comes closest to the fully relaxed **Au20-tilted** conformer that is discussed in the main article.
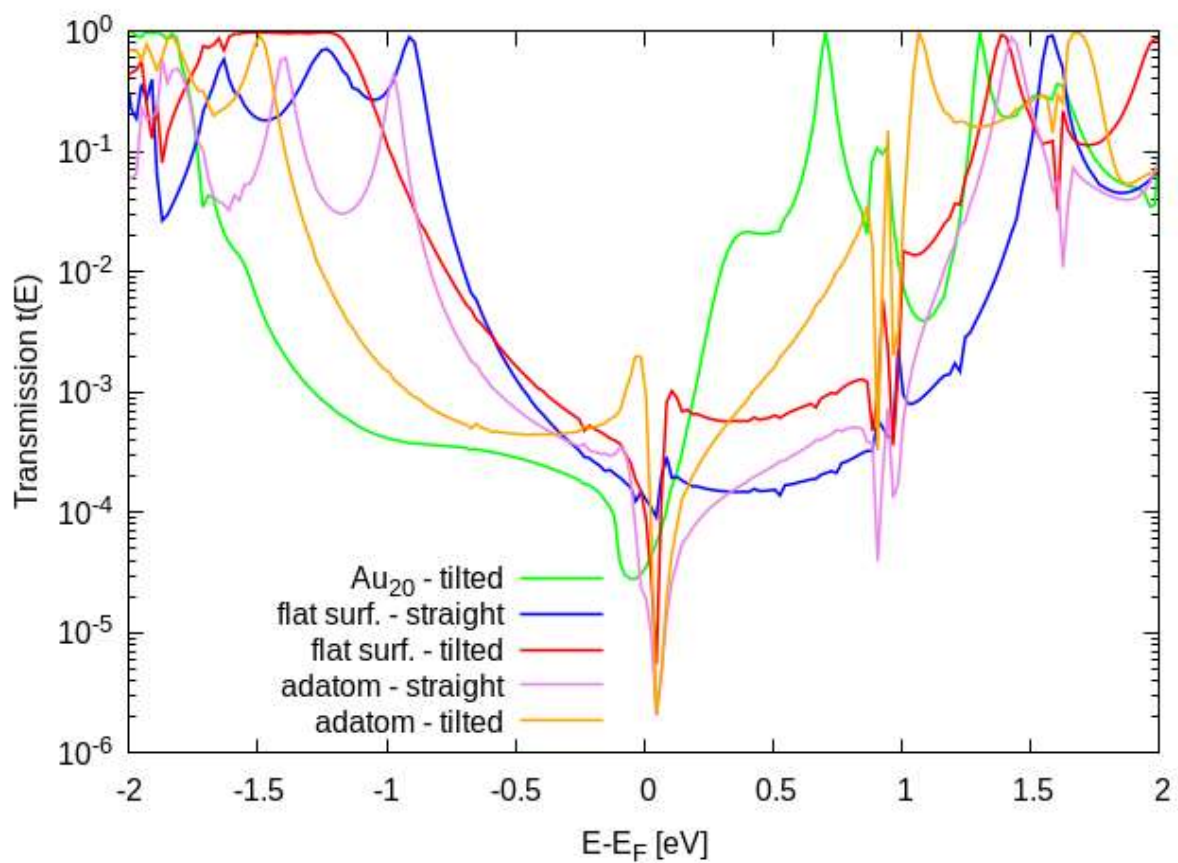
Figure 16. DFTB transmission for **OPE3-Ph** junction models depicted in Fig. 15 and the **Au20-tilted** structure of the main article

VI) Electrical and thermal schematic for Seebeck measurement

As the STM-tip is connected to the voltage source through a copper wire that experiences an opposite temperature gradient, the Seebeck coefficient of the whole junction is given by:

$S_{measured} = S_{molecule} + S_{Cu\text{-}lead}$, with $S_{Cu\text{-}lead} = 1.8$ mV/K [1,2]
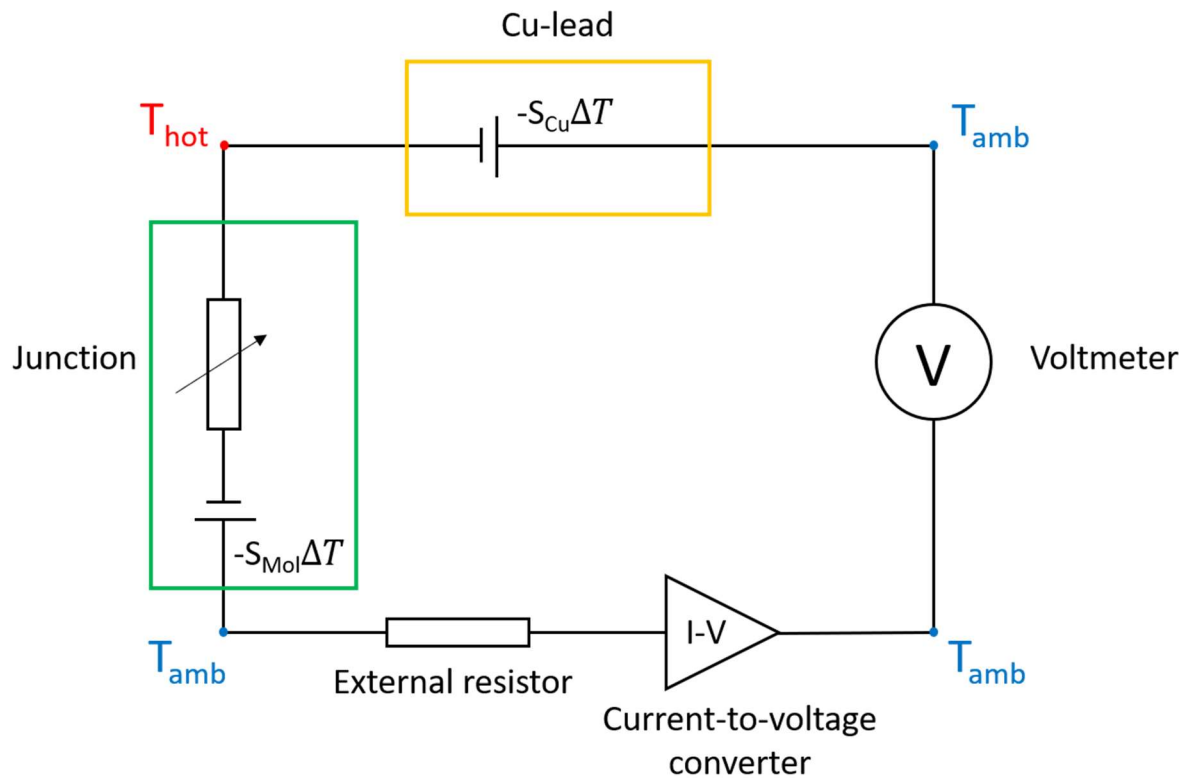
Figure 17. Electrical circuit and equivalent thermal circuit when V_{bias} is set to zero. The molecular junction (marked in green) is electrically equivalent to a conductance G and a thermovoltage (battery) in series. It is also necessary to include the thermovoltage that develops across the connecting copper lead (marked in yellow), due to the uncompensated temperature gradient.

References

1. N. Cusack and P. Kendall, *Proc. Phys. Soc.*, 1958, **72**, 898–901.

2. L. Abadlia, F. Gasser, K. Khalouk, M. Mayoufi and J. G. Gasser, *Rev. Sci. Instrum.* 2014, **85**, 095121.